



Effects of Altitude and Temperature on the Performance and Efficiency of Turbocharged Direct Injection Gasoline Engine

S. Motahari¹ and I. Chitsaz^{2†}

¹ School of Mechanical Engineering, Sharif University of Technology, Tehran, Iran

² Department of Mechanical Engineering, Isfahan University of Technology, Isfahan 84156-83111, Iran

†Corresponding Author Email: ichitsaz189@gmail.com

(Received November 22, 2018; accepted March 2, 2019)

ABSTRACT

Iran is located at the high altitude region and has a diverse four season climate. The temperature difference of two locations at the same time reaches to 50° C. Therefore, the modern direct injection turbocharged engines are highly affected at this condition. This paper deals with the effects of temperature and pressure variations on the engine performance and fuel consumption of turbocharged gasoline direct injection engine. Ford ecoboost is selected for this study and the base experiments are performed at the sea level. At the next step, a comprehensive one-dimensional model of the engine is constructed in GT power and validated with experimental data. Validated model is implemented to investigate the effects of ambient air variations on the engine performance and fuel consumption. The simulations revealed that low end torque is not highly affected by the temperature increase due to the turbocharging compensation while engine torque is significantly dropped at high engine speeds in the elevated temperatures. At constant air temperature, brake specific fuel consumption is decreased for higher intake pressure up to 3000 rpm and does not change up to 3500 rpm.

Keywords: Temperature variations; Altitude effects; Turbocharged; GT power.

NOMENCLATURE

BMEP	Brake Mean Effective Pressure	T_0	stagnation temperature
BSFC	Brake Specific Fuel Consumption	V	speed
BSEC	Brake Specific Energy Consumption		
c	speed of sound		
CA	Crank Angle	η	efficiency
C_p	heat capacity at constant pressure	γ	specific heat ratio
D	diameter of runners		
IMEP	Indicated Mean Effective Pressure λ		ratio of the actual air/fuel to stoichiometric
l	length of runners	μ	coefficient of friction
m	mass	ω	angular velocity
ON	Octane Number	τ	autoignition delay
p	ambient pressure	θ	crank angle
P_0	stagnation pressure	σ	Stefan–Boltzmann constant
Q	heat flux		
SI	spark ignition		
T	temperature		

1. INTRODUCTION

Reducing engine volume (downsizing) offers the potential to meet future emission standards and reduced fuel consumption (2016, 2004). Many

leading companies have introduced their downsized turbocharged engines and this overwhelming popularity is growing fast. The fuel consumption and emission is improved by downsizing in part and medium load while the engine's potentials at full

load is decreased due to the knock sensitivity. Fuel octane number, inlet air temperature and pressure are key factors that significantly affects on knock phenomena (1988).

Major Iranian cities are located above 1300 m above sea level where the engines in the market are not calibrated as well as sea level. Therefore, engine performance is highly affected in this condition. Fig. 1 shows the altitude above sea level for some Iranian cities.

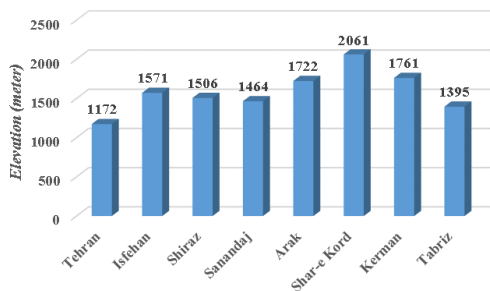


Fig. 1. Altitude above sea level for some Iranian cities.

Iran also is a vast country and has different types of climate: continental and arid in the plateau, cold in high mountains, desert and hot in the southern coast and in the southeast. The maximum temperature of some Iranian cities is shown in Fig. 2.

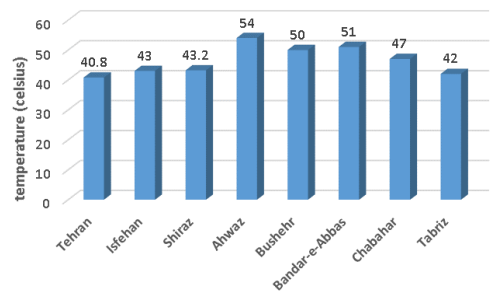


Fig. 2. Maximum temperature of some Iranian cities.

Therefore, the downsized turbocharged engines are affected by the high temperature and altitude in Iran. Many researchers have studied the effects of altitude on the engine performance. *Bielaczyc et al. (2011)* studied the effects of temperature on diesel and SI engines and concluded that the fuel consumption of diesel engines at $-7\text{ }^{\circ}\text{C}$ may be comparable with SI fuel consumption at $24\text{ }^{\circ}\text{C}$. Intake air temperature was also investigated on HCCI engine by *Cinar et al. (2015)*. Intake air temperature was changed from $40\text{ }^{\circ}\text{C}$ to $120\text{ }^{\circ}\text{C}$ and improvement in engine efficiency up to $70\text{ }^{\circ}\text{C}$ was observed but specific fuel consumption was increased after that.

Sakunthalai et al. (2014) investigated the effect of cold ambient conditions on the diesel engine's performance and the exhaust emission. The temperature varied from $-20\text{ }^{\circ}\text{C}$ to $20\text{ }^{\circ}\text{C}$ and the cold start was investigated. The exhaust emissions during the cold start and idle conditions were higher at very cold ambient conditions compared to normal

ambient temperatures. The fuel consumption at cold condition was also higher than normal ambient condition.

Diesel engine emissions have high sensitivity to the altitude and their NOx emission is highly affected at altitude. Therefore, lots of researchers have focused on the emissions of diesel engine at altitude. *He et al. (2011)* performed the experimental study to investigate the effects of altitude on the pollutant emissions of a diesel engine. Their experiments showed the considerable increase in HC, CO and soot. *Wang et al. (2013a)* investigated a heavy duty diesel engine at the altitude of 4500 m which was fueled with diesel and biodiesel. Experimental results revealed that biodiesel operations increased BSEC. They also investigated the effects of altitude on the brake thermal efficiency of heavy duty diesel engine in another study (2013b). Brake thermal efficiency at four altitudes, including sea level, 1600 m, 3300 m and 4500 m was tested. The results indicated that brake thermal efficiency at various altitudes dropped with the rising of altitude; especially for the low speed, low-load cases. *Liu et al. (2014)* investigated the effects of altitude in combination of oxygenated fuel on the performance of diesel engine. They concluded that the diesel fuel at atmospheric condition had the best BSFC. *Szedlmayer and Kweon (2016)* tested a heavy duty diesel engine at the simulated altitude of sea level, 1524, 3048, and 4572 m. Holding BMEP constant at each altitude, resulted in 8% reduction in thermal efficiency at high load and high altitude. A light duty vehicle was used to investigate the effects of altitude and alternative fuels on the performance and emission of diesel vehicle by *Ramos et al. (2016)*. NOx emissions at the altitude was reported around ten times higher than the limits established by the Euro standards. *Pan et al. (2015)* investigated the effects of intake air temperature and methanol fumigation effects on diesel engine performance. In dual fuel operation, the engine thermal efficiency was decreased by reduction in intake air temperature.

Gasoline engines are also sensitive to the altitude and temperature but in a different way. The intake air pressure and temperature directly affects on engine knock limits and the engine management retards the spark time to control the knock. *Wu et al. (2005)* implemented neural network model to compensate the effects of altitude on the air flow rate of combustion engine to reduce cost and time of experimental effort. The effects of fuel sensitivity and altitude on the control parameters of modern production vehicles have been investigated by *Bell (2010)*. Comprehensive testing was performed at an altitude over 1500 meters and confirmatory testing performed near sea level in this research. *Watanabe and Kuroda (1981)* investigated the effect of inlet air temperature on the power output of two-stroke crankcase compression gasoline engine. An inverse relationship between the engine power and the temperature was reported by them. It is also notable that due to their experimental imitations, the temperature range of 273K to 313K was investigated. *Harari and Sher (1993)* also investigated the effects of air pressure on the

performance of a spark ignition two-cylinder two-stroke engine for the aviation applications. They found that at the low engine speeds, engine torque decreased as the inlet air pressure decreases. [Sodre and Soares \(2002, 2003\)](#) investigated the effects temperature, pressure and humidity on the SI engine experimentally on the vehicle. They proposed power correction correlations and compared to existed standards. [Schmick \(2011\)](#) developed a test bed for studying the effects of air temperature and pressure on the small SI engines used in drones. [Husaboe et al. \(2013, 2014\)](#) investigated the effects pressure and temperature variations on the performance of small SI engine. Results revealed a decrease in performance of nominally 4% per 300 m of elevation due to pressure while improvements of 1% per 300 m due to temperature effects. The effects of air intake pressure on the engine performance and emission of single cylinder SI engine was investigated by [Abdullah et al. \(2013\)](#). In this case, they did not change the altitude but remove air filter box to improve pressure drop and increase intake air pressure. The effects of environmental conditions on the spark assisted compression ignition engines was investigated by [Mendrea et al. \(2015\)](#). They reported that the higher ambient temperature makes to advance combustion phasing, while higher humidity makes to retard combustion phasing. Effects of altitude, humidity and temperature on the turbocharged SI engine was investigated by [Amiel and Tartakovsky \(2016\)](#). They simulated four cylinder boxer engine which is implemented in aviation industry and the effects of independent variables on knock was reported. [Rahimi-Gorji et al. \(2017\)](#) investigated the effects of the air pressure and temperature on the power and fuel consumption of SI engine. They implemented GT power to train a neural network and the engine outputs were estimated in terms of variation in air condition.

Altitude variation in Iranian plateau leads to a relatively large difference in ambient pressure and the power output drops drastically. One of the most common methods of engine power keeping at high altitude is turbocharging. The latter compensates for the air density losses and expands the ability of the engine to operate at high altitudes and also to improve the BSFC. The disadvantage of this method is the raise in sensitivity to knock occurrence due to higher temperatures after the compressor. This problem is exacerbated with high temperature in summer, because the decrease in air density results in higher compressor pressure ratios. The range of the possible change in ambient pressure and temperature is wide and therefore, the chance of encountering a combination of parameters that will provoke knock is higher. This study was performed to identify and classify the various parameters and their combinations critical to appearance of knock in SI turbocharged engines in the Iran's environmental condition and to suggest an approach that will allow assessing joint influence of those parameters on knock appearance. The base experiment was done at the sea level laboratory and then, simulation was validated with the experimental data. A comprehensive one-dimensional model of the real

engine was constructed in GT power, and a set of different environmental conditions were implemented to the model. Inlet air temperature and pressure were varied from -10 °C to 50 °C and 0.7 to 1.0 bar, respectively. The engine brake torque, specific fuel consumption and spark time are presented to understand the effects of variation in intake air condition.

2. EXPERIMENTAL SETUP

In this paper, the experiments is conducted on the three cylinder turbo charged direct injection gasoline engine (Ford ecoboost). The overview of main characteristics of this engine is shown in Table 1.

Table 1 Ford ecoboost engine properties

Displacement (liter)	999 cc
Valvetrain	Double overhead camshaft
Number of valve for each cylinder	4
Bore × Stroke	71.9 mm × 82 mm
Bore/Stroke ratio	0.88
Bore pitch	78 mm
Compression ratio	10:1
Maximum torque/power	170 Nm @1750-4500 rpm/88 kW @ 6000 rpm

Experimental setup is shown in Fig. 3. AVL APA 1F4-E-0509 dynamometer is implemented to measure torque and power. Emission measurement of exhaust gases has been provided by Horiba Mexa-700 apparatus.

Fuel mass flow rate is measured by AVL 733s flow meter. To calibrate the numerical model, several thermocouples and flowmeters are installed on the engine test rig. The test rig is shown schematically in

Fig. 4. To measure the IMEP, incylinder pressure sensor is implemented and installed on the cylinder head. Air conditioning system is implemented to exert sea level pressure on the engine intake and exhaust system. The intake air temperature is also monitored and controlled via air conditioning system. Water cooled intercooler is implemented to cool down the intake air temperature and is located in the intake air passage.

The Iranian premium fuel is selected for the experiments and its properties are shown in Table 2.

Table 2 Fuel properties

Octane number	95
Number of carbon in molecule	7.3
Number of hydrogen in molecule	12.09
Low heating value	43.84 MJ / kg
Critical temperature	568.8 K
Critical pressure	24.9 bar



Fig. 3. AVL APA 1F4-E-0509 dynamometer and other accessories.

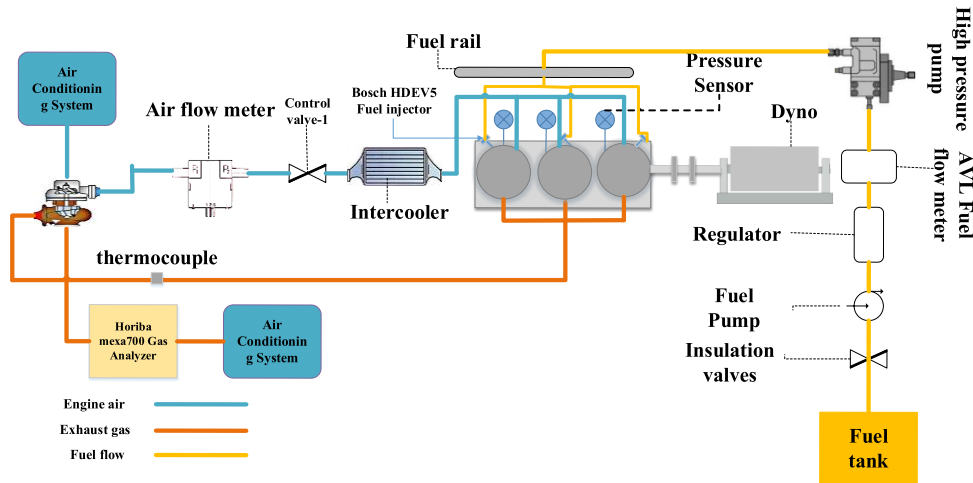


Fig. 4. Schematic of experimental setup.

3. ENGINE MODEL

The 1D engine model is implemented to evaluate the effects of different boundary conditions. Simple finite heat release model is used to calculate incylinder heat release. In this method, heat release rate is calculated using Weibe function (2015). By employing ideal gas equation and Weibe function, correlation between cylinder pressure and crank angle is obtained as is shown in Eq. (1)(1988):

$$\frac{dP}{d\theta} = -\gamma \frac{P}{V} \frac{dV}{d\theta} + \frac{\gamma-1}{V} \left(\frac{\delta Q}{d\theta} \right) \quad (1)$$

Heat transfer from cylinder is calculated by Eq. (2) which is the summation of radiative and convective heat transfers(1988):

$$\dot{Q} = h_c A (T_{wall} - T_g) + \beta \sigma (T_g^4 - T_{wall}^4) \quad (2)$$

β in Eq. (2) equals to 0.6 and T_g is the average temperature of incylinder gas. Convective heat transfer coefficient is calculated by Woschni (1988) correlation:

$$h_c = 3.26 B^{-0.2} p^{0.8} T^{-0.55} w^{0.8} \quad (3)$$

Implementing the first and second laws of thermodynamic as well as Euler equations (1988), turbocharger flow properties is formulated by Eq. (4):

$$\left(\frac{p_{02}}{p_{01}} \right)^{\frac{\gamma_c-1}{\gamma_c}} - 1 = \eta_{CTT} \eta_{TTT} \eta_m \frac{c_{p,T}}{c_{p,C}} \left[1 - \left(\frac{p_4}{p_{03}} \right)^{\frac{\gamma_T-1}{\gamma_T}} \right] \frac{T_{03}}{T_{01}} \quad (4)$$

Where:

η_m = mechanical efficiency

η_{CTT} = isentropic total to total efficiency for compressor

η_{TTT} = isentropic total to total efficiency for turbine

Indexes 1 and 2 in Eq. (4) indicate upstream and downstream parameters of turbine and indexes 3 and 4 refer to upstream and downstream parameters of compressor respectively.

Pressure loss due to gas friction is computed by Bernoulli equation (Eq. (5))and it is assumed that velocity and static head are constant along the pipes (2013):

$$\Delta p = f \frac{l}{D} \frac{\rho V^2}{2} \quad (5)$$

Where f is friction factor which can be determined experimentally or can be read from Moody diagram. Air intake mass flow rate is measured by Eq. (6) (2015):

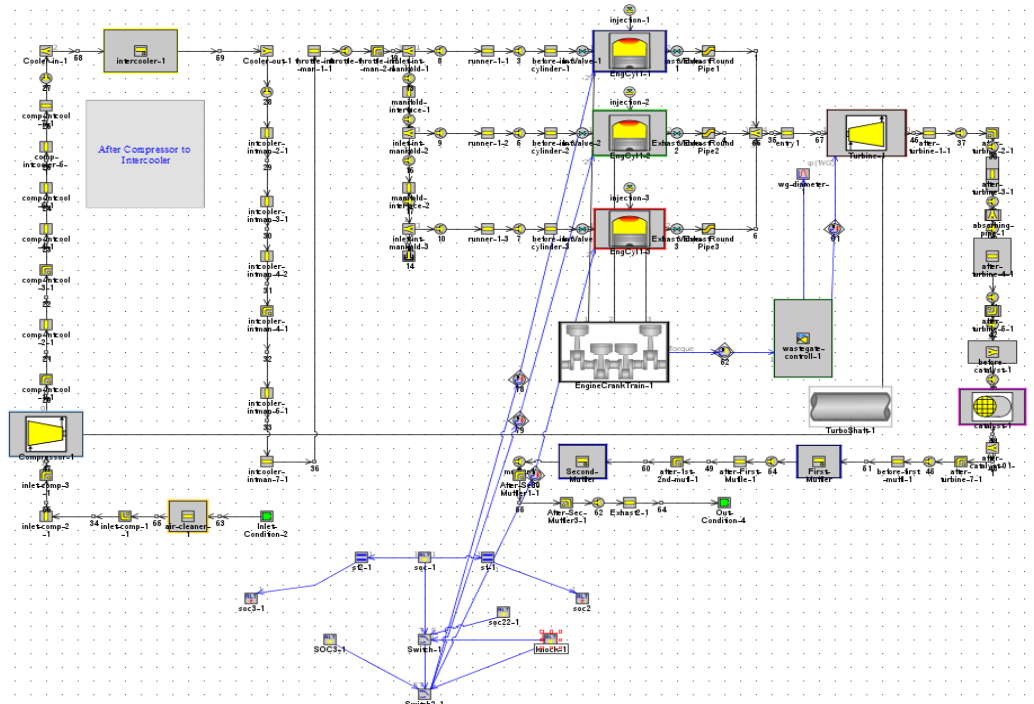


Fig. 5. One dimensional engine model in GT-suite software.

$$m_i = \frac{1}{\omega} \int_{\theta_{i0}}^{\theta_{ic}} m d\theta = \frac{1}{\omega} \int_{\theta_{i0}}^{\theta_{ic}} A_f \rho_c \left[\frac{2}{\gamma-1} \left(\left(\frac{p_v}{p_0} \right)^\gamma - \left(\frac{p_v}{p_0} \right)^\frac{\gamma+1}{\gamma} \right) \right]^{0.5} d\theta \quad (6)$$

Where θ_{i0} is the crank angle when intake valve opens and θ_{ic} is crank angle when intake valve closes, c is the speed of sound, A_f effective intake flow area which is calculated by multiplication of flow coefficient (C_f) in intake flow area. All parameters are computed for charge and discharge conditions. Volumetric efficiency is calculated by Eq. (7)(2015).

$$\eta_v = \frac{m_i}{\rho_i V_d} = \frac{1}{\omega V_d} \int_{\theta_{i0}}^{\theta_{ic}} A_f \frac{\rho}{\rho_i} c \left[\frac{2}{\gamma-1} \left(\left(\frac{p_v}{p_0} \right)^\gamma - \left(\frac{p_v}{p_0} \right)^\frac{\gamma+1}{\gamma} \right) \right]^{0.5} d\theta \quad (7)$$

Where air density in plenum is represented by ρ_i . Autoignition model is utilized to predict knock phenomena. Ignition delay is given by Eq. (8)(2015):

$$\tau = ce \left(\frac{-b}{T} \right) p^n \quad (8)$$

Where n , b and c are empirical constant and dependent on the fuel characteristics. These constants for gasoline is proposed by Douaud and Eyzat (1978):

$$c = 0.01869 \left(\frac{ON}{100} \right)^{3.4017}, n = 1.7, b = 3800$$

Thanks to these coefficient, ignition delay can be precisely predicted. Knock phenomena happen when the Eq. (9) is satisfied (1955):

$$\int_{t=0}^{t=t_c} \left(\frac{1}{\tau} \right) dt = 1 \quad (9)$$

The simulations are conducted by GT-Suite software. One dimensional engine model is designed and then verified. All different parts of the engine such as injectors, turbocharging components and pipes are modeled which are shown in Fig. 5. Flow coefficient and discharge coefficient of intake and exhaust valves used in the model are calculated by steady flow test bench on real engine valves. Turbocharger map is also extracted from turbocharging test bench. A knock controller has been added to the model which is shown in Fig. 6 to investigate the effects intake air temperature and pressure variation on engine output and fuel consumption. Spark time is modified at knock onset according to knock integral calculation. In order to have precise prediction, spark time is retarded by 0.5 degrees of crank angle in each cycle at the occurrence of engine knock.

4. RESULTS AND DISCUSSIONS

In cylinder pressure versus crank angle is shown and validated by experiments in Fig. 7. The numerical

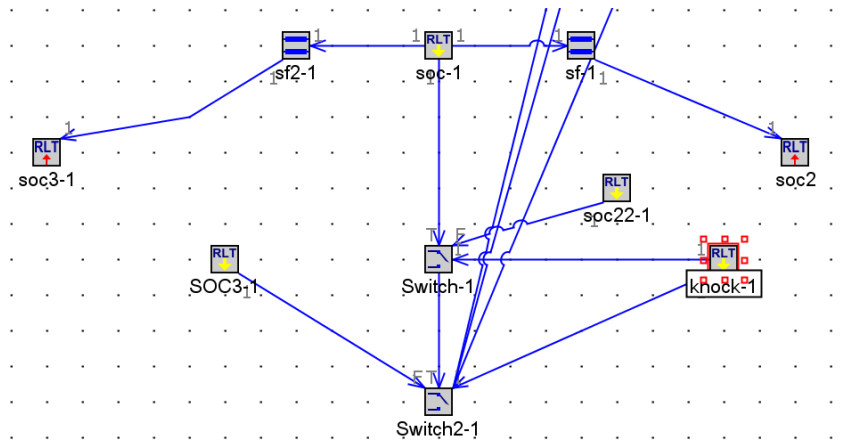


Fig. 6. Knock controller model.

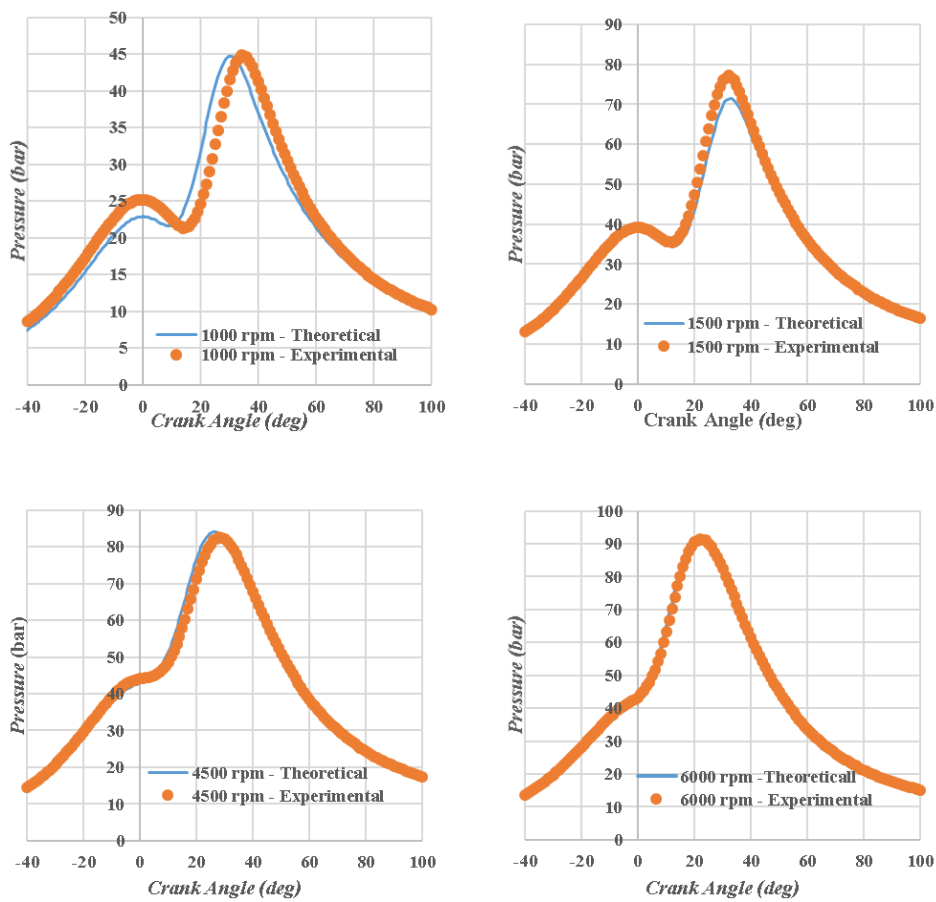


Fig. 7. Pressure versus crank angle diagram for different engine speed, experiment (dots) and numerical result (solid line) at full load condition.

data is validated in different engine speeds to ensure the accuracy of model. As is shown, there is a good agreement between experimental and numerical results. According to the presented results, the maximum error is about 7% for 1500 rpm and average deviation is around 2.8 %.

What is more, Table 3 provides breakdown pertinent to comparison between empirical and numerical

simulation at 1500 rpm.

Based on a reliable GT model that is validated with experiments, the effects of ambient conditions on engine performance and fuel consumption are investigated by the numerical model. Therefore, the upcoming presented results are numerical.

The effects of intake air temperature on the engine fuel consumption and torque are shown in Fig. 8 and

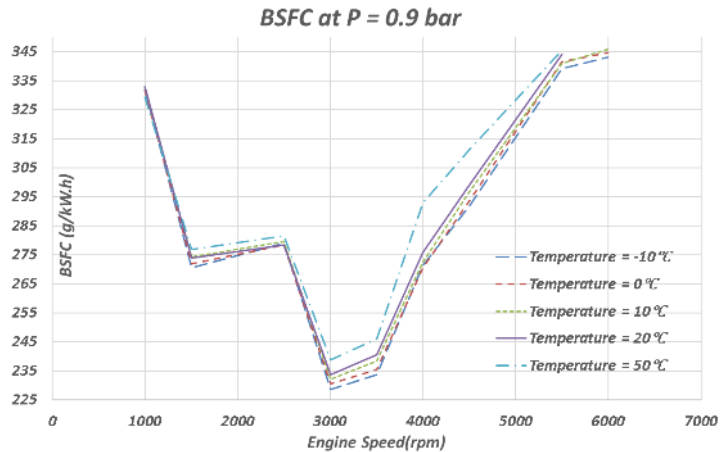


Fig. 8. Specific fuel consumption variation for different intake air temperature at p=0.9 bar and full load.

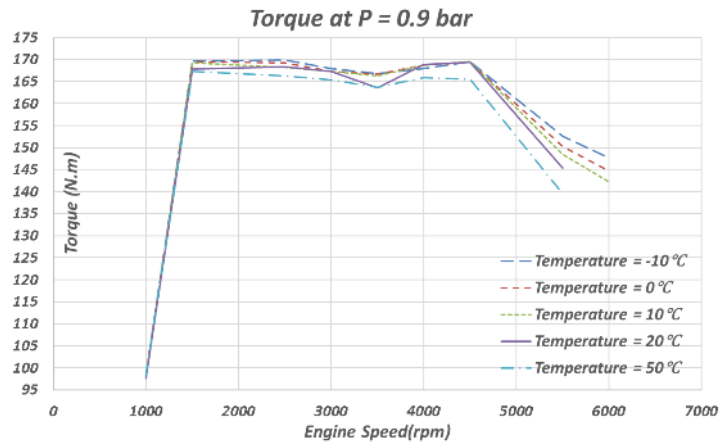


Fig. 9. Engine Torque variation for different intake air temperature at p=0.9 bar and full load.

Fig. 9 respectively for full load condition. As shown in this figure, specific fuel consumption is increased as the intake air temperature increase. This variation is due to the retard of spark time which reduces the engine efficiency and increases the fuel consumption. The fuel consumption increase is intensified in the speed ranges of 3000 to 4500 rpm. At low engine speeds below than 3000 rpm, valve overlap is implemented by engine management to improve volumetric efficiency and engine low end torque. Therefore, lambda is maintained above 1 by valve overlap. At high engine speeds above 4500 rpm, the mixture is enriched by engine management to control the exhaust manifold temperature and lambda is maintained below than 0.9. Lambda at middle engine speed from 3000 to 4500 rpm and full load condition is around 0.9 to 1.0 which is the most probable engine knock condition. Therefore, this range of speed has the highest sensitivity to knock phenomena and is highly affected by temperature increase. As the intake air temperature increases, the probability for engine knock is intensified. Therefore, the spark time is retarded and the engine efficiency is reduced.

Table 3 comparison between empirical and simulation results for 1500 rpm and full load

parameter	Empirical data	Simulation result	Error %
Torque (N.m)	168.55	169.6314	0.64
BMEP (bar)	21.18	21.34191	0.76
BSFC (g/kW.h)	277.7	272.9673	1.7
Volumetric efficiency (%)	256.1	242.937	5.14
lambda	1.225	1.201259	1.94

Engine torque is also affected by the temperature increase. As shown in Fig. 9, the low end torque is not highly affected by the temperature increase due to the turbocharging compensation. Engine torque is significantly dropped at high engine speeds by temperature increase. This is due to the turbocharger speed limit that density reduction of high temperature air cannot be compensated as well as low engine speeds. At the middle engine speeds (2000-4500), torque is also decreased due to the spark timing retard.

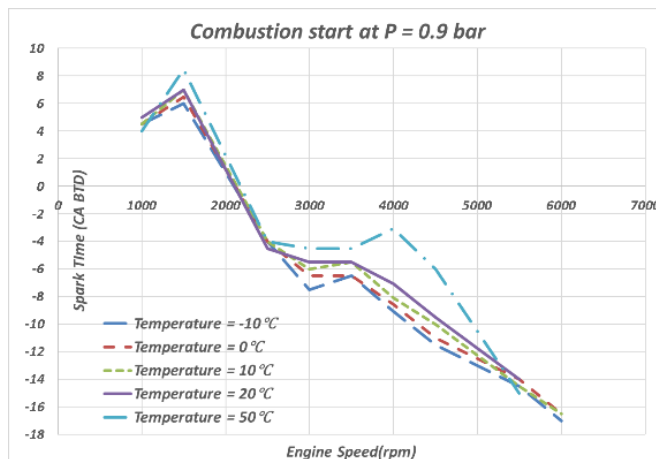


Fig. 10. Spark time variation for different intake air temperature at p=0.9 bar and full load.

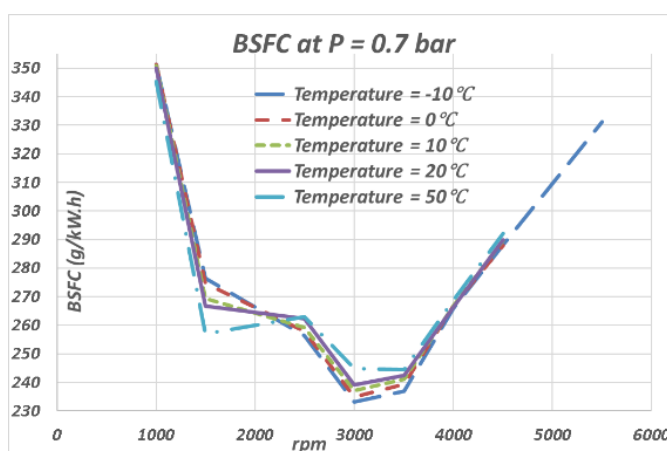


Fig. 11. Specific fuel consumption variation for different intake air temperature at p=0.7 bar and full load.

The spark time variation is also shown in Fig. 10. As shown in this figure, the most change in spark time happens at the middle engine speeds which is due to the fuel air equivalence ratio. This indicates that the spark time is not solely affected by the temperature variation and should be considered along with the air to fuel equivalence ratio.

The effects of temperature variation on BSFC at high altitude are simulated by p=0.7 bar and shown in Fig. 11. As shown in this figure, the overall trend is similar to the p=0.9 bar except for 1500 rpm. The specific fuel consumption for the highest temperature is dropped to minimum BSFC. The intake air density is decreased at the pressure of 0.7 bar and the temperature increase intensifies this reduction. Density reduction reaches the extent that cannot be compensated by the turbocharger. Turbocharger in this condition (high altitude and high temperature) approaches to the surge line and the air mass flow rate is decreased significantly. The lower mass flow rate result in knock suppression. Therefore, spark time is advanced by the controller and the specific fuel consumption is improved. At higher engine speeds, turbocharger is away from the surge line and the density reduction is compensated by the turbocharger. Therefore, the spark time is retarded and the specific fuel consumption has an

increasing trend by temperature increase like p=0.9.

The maximum torque is also shown in Fig. 12. As shown in this figure, the low end torque at 1500 rpm is significantly decreased at high altitude and temperature to as low as 135 Nm. The air density at high temperature and low pressure can not be compensated by the turbocharger and the air mass flow is decreased significantly. Although the spark time can be advanced at low end torque and engine efficiency is improved, but the air mass flow rate is highly decreased to the level that engine torque is dropped significantly. The engine torque has also a little variation from 2500 to 3000 rpm that implies the engine torque is not sensitive to the ambient condition in these engine speeds. This figure emphasizes that the low engine speed at full load condition is more affected than other engine speeds by altitude and temperature.

The spark time at high altitude for different temperatures are shown in Fig. 13. As shown in this figure, high altitude has a similar trend to the p=0.9 except for the 1500 rpm. As described, the air mass flow at 1500 rpm is decreased significantly and the knock probability is reduced. Therefore, the spark time is advanced up to the knock limit in the engine controller. The trend of spark time after 1500 rpm,

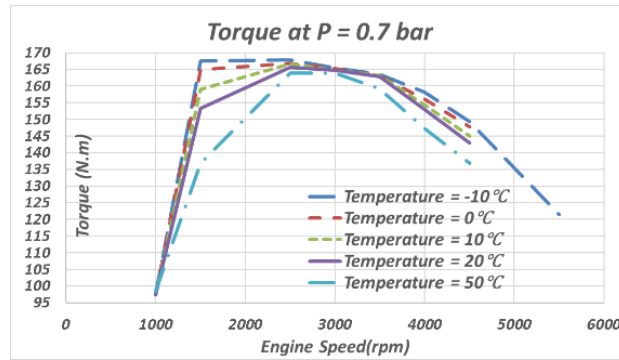


Fig. 12. Engine Torque variation for different intake air temperature at $p=0.7$ bar and full load.

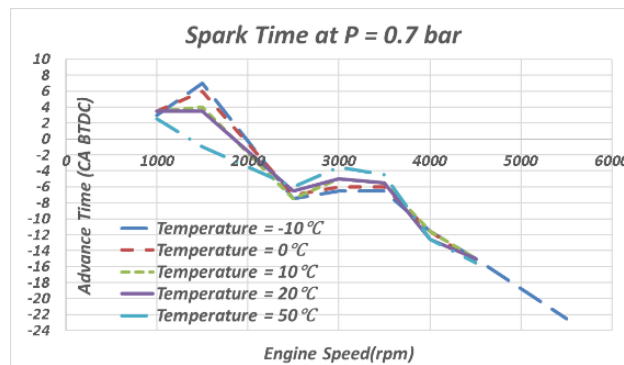


Fig. 13. Spark time variation for different intake air temperature at $p=0.7$ bar and full load.

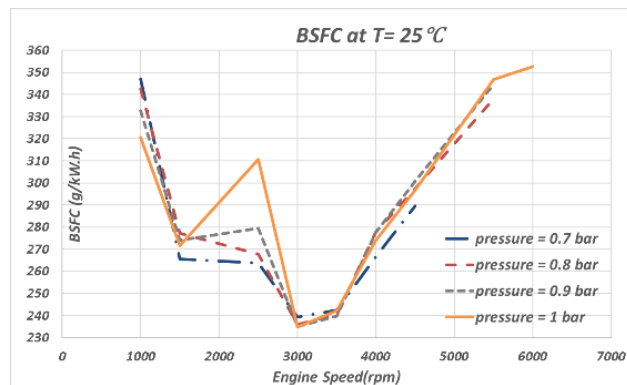


Fig. 14. Specific fuel consumption variations for different altitudes at $T=25$ °C and full load.

returns to the expected trend which is completely similar to $p=0.9$. In this condition, the spark time at higher intake temperatures is retarded more than lower intake temperatures.

To simulate the effects of altitude variations, intake air pressure is varied from 0.7 to 1 bar and the results of BSFC are shown in Fig. 14. As is shown in this figure, BSFC is decreased for higher intake pressure up to 3000 rpm and does not change from this engine speed up to 3500 rpm. The intake pressure at low engine speeds (lower than 3000 rpm) is limited by the turbocharger performance at low intake pressures. The turbocharger performance at low engine speed is limited by its surge line and the low pressure at intake manifold can not be compensated by the turbocharger. Therefore, air mass flow rate is decreased and knock phenomena is suppressed at low pressure condition. The spark time is advanced

by engine knock control and the efficiency is improved. At medium engine speeds (3000-3500rpm) turbocharger performance is deviated from the surge line and the intake air pressure is boosted to an acceptable level in comparison to $p=1$ bar. Therefore, there are no big variations in efficiency for these operating points. At high engine speeds, due to the turbocharger speed limit (216,000 rpm) the air intake mass flow is decreased but not as much as low engine speeds. Therefore, the spark time is advanced for the low air pressure by the knock controller that improves efficiency a little.

Although the engine efficiency improves at the most of engine speeds for high altitude condition, but engine torque is dropped significantly that is shown in Fig. 15. As shown in this figure, the low end torque decreases as the intake air pressure decreases. There is a significant reduction at low end torque for $p=0.7$

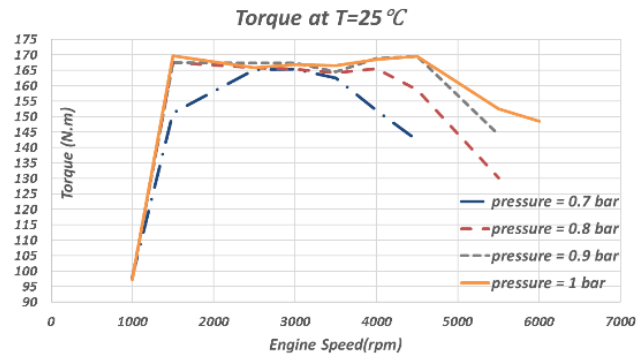


Fig. 15. Engine Torque variations for different altitudes at T=25 °C and full load.

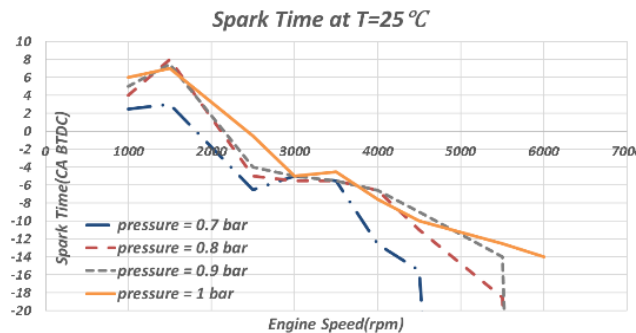


Fig. 16. Spark time variation for different altitude at T=25 °C and full load.

which is due to the turbocharger limitations. The torque at high engine speeds is also reduced by the reduction of air intake pressure. The turbocharger speed limit that is 216000 rpm leads to significant reduction in high speed maximum torque.

The spark time can be advanced if the in cylinder pressure is reduced. Therefore, the spark time for lower intake pressure (higher altitude above sea level) can be advanced except the medium speeds (3000 to 3500 rpm). In the medium engine speeds, the turbocharger is gone away from the borderline and the intake air mass flow is compensated. Aforementioned trend is shown in Fig. 16.

5. CONCLUSIONS

The present study provides the numerical along with experimental study to investigate the effects of intake air temperature and pressure on the engine performance and efficiency. The main goal of this paper is to find the effects of Iran's environmental conditions on the turbocharged engine. Therefore, a numerical model that is validated by experimental data is implemented. Numerical parametric study have been done on the full load condition. Spark time, specific fuel consumption and engine torque are represented as dependent variables to understand the effects of Iran's tough geographic conditions on turbocharged engine.

Lambda at middle engine speeds (from 3000 to 4500 rpm) and full load condition for ecoboost is around

0.9 to 1.0 which is the most probable engine knock condition. Therefore, this range of speeds has the highest sensitivity to knock phenomena and is highly affected by temperature increase. The low end torque is not highly affected by the temperature increase due to the boost compensation while engine torque is significantly dropped at high engine speeds.

The spark time is not solely affected by the temperature variation and should be considered along with the air to fuel equivalence ratio. This parameter is highly affected by engine calibration and may changes form one engine to another engine.

Turbocharger at high altitudes and high temperatures, approaches to the compressor surge line and the air mass flow rate is decreased significantly. Therefore, specific fuel consumption is improved at high altitudes and temperatures while the engine torque is dropped. All turbocharged engines have a similar trend in this condition.

Engine efficiency is decreased for higher intake pressure (at constant air temperature) up to 3000 rpm and does not change up to 3500 rpm. At medium engine speeds (3000-3500rpm), there is no big variation in efficiency due to turbocharger map. The engine torque at high altitudes is also significantly dropped except a limited boundary of engine speed (3000-3500 rpm). This behavior is predictable for all turbocharged engines but the range of middle engine speeds depend on the compressor map.

The spark time is advanced at high altitudes and is

retarded for high intake air temperatures. There is also an exception for high temperatures and high altitudes that the spark time is highly advanced due to reduction of air mass flow rate.

REFERENCES

- Hu, B., S. Akehurst, and C. Brace,(2016) Novel approaches to improve the gas exchange process of downsized turbocharged spark-ignition engines: A review. *International Journal of Engine Research* 17(6): 595-618.
- Lake, T., J. Stokes, R. Murphy, R. Osborne, and A. Schamel,(2004), Turbocharging Concepts for Downsized DI Gasoline Engines, in., *SAE International*.
- Heywood, J. B. (1988) *Internal combustion engine fundamentals*.
- NASA.(Available from: <http://floodmap.net/elevation/countryelevationmap/?ct=IR>.
- weather, I.(Available from: [https:// HYPERLINK](https://HYPERLINK) "http://www.irimo.ir/eng/index.php" www.irimo.ir/eng/index.php
- Bielaczyc, P., A. Szczotka, and J. Woodburn (2011) The effect of a low ambient temperature on the cold-start emissions and fuel consumption of passenger cars. Proceedings of the Institution of Mechanical Engineers, Part D: *Journal of Automobile Engineering* 225(9): 1253-1264.
- Cinar, C., A. Uyumaz, H. Solmaz, F. Sahin, S. Polat, and E. Yilmaz (2015) Effects of intake air temperature on combustion, performance and emission characteristics of a HCCI engine fueled with the blends of 20% n-heptane and 80% isooctane fuels. *Fuel Processing Technology* 130: 275-281.
- Arumugam Sakunthalai, R., H. Xu, D. Liu, J. Tian, M. Wyszynski, and J. Piaszyk (2014) Impact of Cold Ambient Conditions on Cold Start and Idle Emissions from Diesel Engines, in., *SAE International*.
- He, C., Y. Ge, C. Ma, J. Tan, Z. Liu, C. Wang, L. Yu, and Y. Ding,(2011) Emission characteristics of a heavy-duty diesel engine at simulated high altitudes. *Science of The Total Environment* 409 (17): 3138-3143.
- Wang, X., Y. Ge, L. Yu, and X. Feng (2013a) Comparison of combustion characteristics and brake thermal efficiency of a heavy-duty diesel engine fueled with diesel and biodiesel at high altitude. *Fuel* 107: 852-858.
- Wang, X., Y. Ge, L. Yu, and X. Feng (2013b) Effects of altitude on the thermal efficiency of a heavy-duty diesel engine. *Energy* 59: 543-548.
- Liu, S., L. Shen, Y. Bi, and J. Lei (2014) Effects of altitude and fuel oxygen content on the performance of a high pressure common rail diesel engine. *Fuel* 118, 243-249.
- Szedlmayer, M. and C. B. M. Kweon (2016) Effect of Altitude Conditions on Combustion and Performance of a Multi-Cylinder Turbocharged Direct-Injection Diesel Engine, in., *SAE International*.
- Ramos, Á., R. García-Contreras, and O. Armas (2016) Performance, combustion timing and emissions from a light duty vehicle at different altitudes fueled with animal fat biodiesel, GTL and diesel fuels. *Applied Energy* 182: 507-517.
- Pan, W., C. Yao, G. Han, H. Wei, and Q. Wang (2015) The impact of intake air temperature on performance and exhaust emissions of a diesel methanol dual fuel engine. *Fuel* 162: 101-110.
- Wu, B., Z. Filipi, D. M. Kramer, G. L. Ohl, M. J. Prucka, and E. DiValetin,(2005), Using neural networks to compensate altitude effects on the air flow rate in variable valve timing engines, *SAE Technical Paper*.
- Bell, A. (2010), Modern SI Engine Control Parameter Responses and Altitude Effects with Fuels of Varying Octane Sensitivity, *SAE International*.
- Watanabe, I. and H. Kuroda (1981), Effect of atmospheric temperature on the power output of a two-stroke cycle crankcase compression gasoline engine, *SAE Technical Paper*.
- Harari, R. and E. Sher (1993) The effect of ambient pressure on the performance map of a two-stroke SI engine. *SAE Transactions*: 681-689.
- Soares, S. M. C. and J. R. Sodre (2002) Effects of atmospheric temperature and pressure on the performance of a vehicle. Proceedings of the Institution of Mechanical Engineers, Part D: *Journal of Automobile Engineering* 216(6): 473-477.
- Sodré, J. and S. Soares (2003) Comparison of engine power correction factors for varying atmospheric conditions. *Journal of the Brazilian Society of Mechanical Sciences and Engineering* 25(3): 279-284.
- Schmick, P. J. (2011), Effect of Atmospheric Pressure and Temperature on a Small Spark Ignition Internal Combustion Engine's Performance, *Air Force Inst Of Tech Wright-Patterson Afb Oh School Of Engineering And Management*.
- Husaboe, T. D., M. D. Polanka, J. A. Rittenhouse, P. J. Litke, and J. L. Hoke (2014) Dependence of Small Internal Combustion Engine's Performance on Altitude. *Journal of Propulsion and Power* 30(5): 1328-1333.
- Husaboe, T. D. (2013), Effects of Temperature on the Performance of a Small Internal Combustion Engine at Altitude, *Air Force Inst Of Tech Wright-Patterson Afb Oh Graduate School Of Engineering And Management*.
- Abdullah, N. R., N. S. Shahrudin, A. M. I. Mamat, S. Kasolang, A. Zulkifli, and R. Mamat (2013) Effects of air intake pressure to the fuel economy and exhaust emissions on a small SI

- engine. *Procedia Engineering* 68, 278-284.
- Mendrea, B., Y. Chang, Y. Z. A. Akkus, J. Sterniak, and S. Bohac (2015), Investigations of the Effect of Ambient Condition on SACI Combustion Range, *SAE International*.
- Amiel, R. and L. Tartakovsky (2016), Effect of Flight Altitude on the Knock Tendency of SI Reciprocating Turbocharged Engines, *SAE International*.
- Rahimi-Gorji, M., M. Ghajar, A. H. Kakaee, and D. D. Ganji (2017) Modeling of the air conditions effects on the power and fuel consumption of the SI engine using neural networks and regression. *Journal of the Brazilian Society of Mechanical Sciences and Engineering* 39(2): 375-384.
- Ferguson, C. R. and A.T. Kirkpatrick (2015) *Internal combustion engines: applied thermosciences*. John Wiley & Sons.
- Munson, B. R., T. H. Okiishi, W. W. Huebsch, and A. P. Rothmayer (2013) *Fluid mechanics*. Wiley Singapore.
- Douaud, A. and P. Eyzat (1978), Four-octane-number method for predicting the anti-knock behavior of fuels and engines, *SAE Technical Paper*.
- Livengood, J. and P. Wu (1955) Correlation of autoignition phenomena in internal combustion engines and rapid compression machines. in *Symposium (international) on combustion*. Elsevier.